https://doi.org/10.5194/egusphere-2025-3597
Preprint. Discussion started: 13 August 2025

Atmospheric lifetime of sulfur hexafluoride (SF_6) and five other trace gases in the BASCOE model driven by three reanalyses

Sarah Vervalcke[1], Quentin Errera[1], Simon Chabrillat[1], Marc Op de beeck[1], Thomas Reddmann[2], Gabriele Stiller[2], Roland Eichinger[3], and Emmanuel Mahieu[4]

[1]Royal Belgian Institute for Space Aeronomy (BIRA-IASB), Brussels, Belgium
[2]Institute for Meteorology and Climate Research, Karlsruhe Institute of Technology (KIT), Karlsruhe, Germany
[3]Institut für Physik der Atmosphäre, Deutsches Zentrum für Luft- und Raumfahrt (DLR), Oberpfaffenhofen, Germany
[4] Institute of Astrophysics and Geophysics, Université de Liège (ULg), Liège, Belgium

Correspondence: Sarah Vervalcke (sarah.vervalcke@aeronomie.be) and Quentin Errera (quentin.errera@aeronomie.be)

Abstract

In this work, sulfur hexafluoride (SF_6), which is often used as a tracer for stratospheric transport due to its inertness in the stratosphere and nearly linear growth rate in the troposphere, is included in the chemistry transport model (CTM) of the Belgian Assimilation System for Chemical ObsErvations (BASCOE). Sink and recovery reactions for this species are implemented in the model, which has a top in the mesosphere at 0.01 hPa. The simulated SF_6 distributions are compared with MIPAS and ACE-FTS observations and the global atmospheric lifetime is computed from CTM runs driven by three recent meteorological reanalyses: ERA5, MERRA2 and JRA-3Q. The results show that BASCOE SF_6 profiles are generally within 10% of the satellite observations below 10 hPa, although discrepancies increase at higher altitudes. The global atmospheric lifetime is used as an additional diagnostic for the implementation of the chemistry in the mesosphere, where satellite measurements are unavailable. The derived SF_6 lifetimes are 2646 years with ERA5, 1909 years with MERRA2 and 2147 years with JRA-3Q, in accordance with recent literature. Due to the large spread of published lifetimes for SF_6, the study is extended to N_2O, CH_4, CFC-11, CFC-12 and HCFC-22, to validate the SF_6 results. The lifetimes for these species are in agreement with previously reported values, and their spread between simulations is smaller compared to SF_6. This analysis highlights the sensitivity of SF_6 to the input reanalysis data sets and thus to differences in dynamics.

1 Introduction

Studies of middle atmospheric transport have been important for a long time and are motivated by the existence of the stratospheric ozone layer that protects the Earth from solar UV radiation. Transport of trace gases in the middle atmosphere is dominated by a large scale circulation pattern in the stratosphere, called the Brewer-Dobson circulation (BDC), discovered by A. Brewer and G. Dobson (Brewer, 1949; Dobson, 1956; Dobson et al., 1930). The BDC is the result of an uplift of air from the tropical tropopause into the stratosphere and a consequent poleward transport driven by planetary wave breaking in the atmosphere. At mid- and high latitudes the air returns to the troposphere upon which it can be recirculated. The BDC is important for the transport of trace gases such as ozone, influencing both the chemistry and climate of the atmosphere. A comprehensive review of the Brewer-Dobson circulation can be found in Butchart (2014).

https://doi.org/10.5194/egusphere-2025-3597
Preprint. Discussion started: 13 August 2025

General climate models predict an increase in the strength of the BDC (Butchart and Scaife, 2001; Butchart et al., 2006; Garcia and Randel, 2008; Calvo and Garcia, 2009; McLandress and Shepherd, 2009), typically quantified by the tropical mass upwelling. While strength and speed describe different aspects of the circulation, they tend to vary together, as shown by Austin and Li (2006). A common way to diagnose the speed of the BDC is through age of air (AoA) studies. These studies look at the (average) time an air parcel takes to move from a reference surface in the troposphere to the stratosphere. Changes in AoA thus reflect changes in circulation speed: the transportation time increases when the circulation slows down and decreases when the circulation speeds up. Additionally, two-way mixing influences stratospheric AoA, partly through making air parcels recirculate (Garny et al.; Dietmüller et al.; Eichinger et al.). The concept of AoA is described in Hall and Plumb (1994), Waugh and Hall (2002), Garny et al. (2024) and Saunders et al. (2025). The AoA can be computed from a synthetic, idealized model tracer or from real long-lived trace gases with a nearly linear increase in the troposphere, such as carbon dioxide (CO_2) and sulfur hexafluoride (SF_6). SF_6 in particular is often used because of its inertness in the stratosphere and the absence of strong seasonal variations. The emissions of SF_6 at the surface are almost completely anthropogenic due to its use in high voltage insulation for the transmission and distribution of electricity. Additionally, SF_6 is a potent greenhouse gas with a global warming potential (GWP) that is estimated to be 22,500 times the GWP of CO_2 (Wang et al., 2019) and is therefore important for climatological studies.

While AoA trends are a useful diagnostic, discrepancies exist between AoA trends computed from observations, models and reanalyses (Chabrillat et al., 2018; Ploeger et al., 2019; Garny et al., 2024). In this work, the implementation of SF_6 in the Belgian Assimilation System for Chemical ObsErvations (BASCOE) chemistry transport model (CTM) is described. The implementation of SF_6 is evaluated using independent satellite observations from MIPAS and ACE-FTS, and via the computation of the global atmospheric lifetime of SF_6, which is compared with the literature. Three recent meteorological reanalyses have been used to drive the BASCOE simulations: ERA5, MERRA2 and JRA-3Q. These reanalyses extend upwards to 0.01 hPa in the mesosphere where SF_6 chemistry is important. In this study we use three different sets of reanalysis data to drive the BASCOE model in order to analyse the influence of the meteorology on the results. Due to a large spread of the lifetime values, both those presented here as well as those found in the literature, the work was extended to five other long-lived species to support the evaluation of our methods and results: N_2O, CH_4, CFC-11, CFC-12 and HCFC-22. These six species can be used to compute the AoA using the method from Voet et al. (2025). However, AoA diagnostics are not presented in this work.

The paper is organised as follows: Section 2 introduces the different data sets used. This includes MIPAS and ACE-FTS observations and the three reanalyses. Section 3 discusses the BASCOE model simulations, and in particular the implementation of the chemistry of SF_6 and the set-up of the model. Section 4 describes the computation of the global atmospheric lifetime. Finally, the comparison between the model simulations and the observations is presented in Sect. 5, along with the obtained values for the global lifetime. The conclusions are presented in Sect. 6. While this study compares diagnostics of the reanalyses, it does not present a full inter-comparison of the reanalyses themselves.

https://doi.org/10.5194/egusphere-2025-3597
Preprint. Discussion started: 13 August 2025

2 Data sets

The following sections describe the data sets that are used in this work. The first two subsections deal with the satellite data that are used to evaluate the model results. The last subsection informs about the reanalysis data sets that are used as input for the BASCOE CTM. We used two satellite data sets as observational reference, namely MIPAS and ACE-FTS. These are described in more detail below. As drivers for BASCOE, three different reanalyses were used, namely ERA5, MERRA2, and JRA-3Q. Details about these reanalyses are given below.

2.1 MIPAS

The Michelson Interferometer for Passive Atmospheric Sounding (MIPAS, Fischer et al., 2008), onboard the ENVISAT satellite, operated from July 2002 until April 2012 in a sun-synchronous low-Earth orbit. It is a Fourier Transform Spectrometer with a limb viewing geometry, measuring atmospheric infrared radiation from which vertical profiles of trace gases are retrieved. MIPAS was designed to measure over 20 species, including SF_6, CFC-11 and CFC-12, CH_4, N_2O and HCFC-22. In April 2004, MIPAS had a failure and observations were halted until January 2005, after which measurements resumed with reduced spectral resolution. MIPAS datasets are thus typically split into two phases: one with high spectral resolution and one with reduced spectral resolution. In this study, MIPAS data from the IMK/IAA research processor are used to evaluate the model output. The MIPAS data versions that are used in this work are summarized in Table 1. To judge the model bias with respect to MIPAS and ACE-FTS observations, we compare with typical uncertainties from satellite validation studies. The uncertainties from available validation studies with various, sometimes older, versions are also shown in Table 1. Most of the instrument biases between ACE-FTS and MIPAS are between 10 and 20%, particularly for the species CH_4, N_2O and CFC-12. However, the agreement depends on the altitude and biases increase significantly above 50 hPa for some species.

2.2 ACE-FTS

The Atmospheric Chemistry Experiment Fourier Transform Spectrometer (ACE-FTS) is a Canadian-led mission on SCISAT-1 (Bernath et al., 2005). It started taking measurements in February 2004 and is still operational after more than 20 years on orbit. This instrument performs infrared solar-occultation measurements on an inclined circular orbit. ACE-FTS takes measurements twice per orbit, during sunrise and sunset, allowing for up to 30 observations per day. ACE-FTS focuses on the region in the stratosphere that contains the ozone layer and measures 70 atmospheric trace gases, including CFC-11, CFC-12, CH_4, N_2O and HCFC-22. The data version used in this work is V5.3.

2.3 Reanalyses

Three different reanalysis data sets are used to drive the BASCOE chemistry transport model. Reanalyses offer a globally complete data set of atmospheric variables by assimilating observational data into models to ensure spatial and temporal homogeneity. Reanalyses with a top around 0.01 hPa were chosen to capture mesospheric circulation features that are important for the chemistry of SF_6.

https://doi.org/10.5194/egusphere-2025-3597
Preprint. Discussion started: 13 August 2025

Table 1. Summary of measurement uncertainties for ACE-FTS and MIPAS from validation studies.

Species	Compared instruments	Agreement	Notes and References	Data versions in this work
SF_6	ACE-FTS V2.2, MIPAS spectral version 5	Good, below 50 hPa. Above 50 hPa, mostly within ±5%, some regions ±10% to ±20%	Annual zonal mean profiles below 50 hPa agree well; monthly means vary by level (SPARC, 2017).	MIPAS IMK/IAA V8, ACE-FTS V5.3
N_2O	ACE-FTS V3.5, MIPAS spectral version 5, MLS V3.3	-20% to +10%	Observed uncertainties from MLS and MIPAS (Sheese et al., 2017).	MIPAS IMK/IAA V8, ACE-FTS V5.3
CFC-11	ACE-FTS V2.2, MIPAS spectral version 5	Good, below 100 hPa (5-10%). Up to 50% above 100 hPa.	Agreement decreases above 100 hPa (SPARC, 2017).	MIPAS IMK/IAA V8, ACE-FTS V5.3
CFC-12	ACE-FTS V2.2, MIPAS spectral version 5	Good agreement. Uncertainties within ±10% across the vertical range.	SPARC (2017).	MIPAS IMK/IAA V8, ACE-FTS V5.3
CH_4	ACE-FTS V3.5, MIPAS spectral version 5	Good (12% between 20-65 km). Bias of 15% at 17 km	MIPAS shows largest VMRs at 17 km (Laeng et al., 2015).	MIPAS IMK/IAA V8, ACE-FTS V5.3
	ACE-FTS V2.2, HALOE V19, MIPAS spectral version 5	±20% agreement.	Across entire vertical range, good agreement (SPARC, 2017).	
HCFC-22	ACE-FTS V5.2, MIPAS IMK/IAA V8	+3 to 10 % bias between 5 and 10km. ±5 % bias between 10 and 21 km. +5 to 14 % bias between 21 and 25 km.	Agreement varies with altitude (Kolonjari et al., 2024).	MIPAS IMK/IAA V8, ACE-FTS V5.3

The first reanalysis is the ERA5 (Hersbach et al., 2020) data set, issued by the European Centre for Medium-Range Weather Forecasts (ECMWF). It is available from 1940 onwards. The ERA5 atmospheric data has a horizontal resolution of 31km (∼0.28125°), and 137 vertical levels from the surface up to 0.01hPa.

Similarly, the Modern-Era Retrospective analysis for Research and Applications, or (MERRA2, Gelaro et al., 2017), is a data set from the Global Modelling and Assimilation Office (GMAO) which covers the period 1980 to present. The data set has a horizontal resolution of 0.5°x0.625° and 72 vertical levels, from the surface up to 0.015 hPa. MERRA2 is the only one of the three reanalysis data sets used here that assimilates Aura Microwave Limb Sounder (Aura MLS) temperature profiles from 2004 onwards above 5 hPa (SPARC, 2022).

https://doi.org/10.5194/egusphere-2025-3597
Preprint. Discussion started: 13 August 2025

Finally, the Japanese Reanalysis for Three Quarters of a Century (JRA-3Q, Kosaka et al., 2024) is the third long-term reanalysis produced by the Japan Meteorological Agency (JMA), covering the period from September 1947 to present. This is the most recently released data set of the three reanalyses used in this work. JRA-3Q has a higher resolution than its predecessor JRA-55: it has a horizontal resolution of 40km ($\sim 0.359°$) and 100 vertical levels from the surface to 0.01hPa.

Each reanalysis has a sponge layer at the model top to avoid unphysical reflection of wave energy at a rigid model lid. These sponge layers are implemented differently in each reanalysis and can explain some of the differences found at the upper levels and in our results. According to SPARC (2022, Chap. 5) the climatological wave driving and the climatological circulation strength and structure agree closely among the most recent reanalysis products available at the time (MERRA2, ERA5 and JRA-55), however, MERRA2 is shown to have slower upwelling in the tropics than the other reanalyses. This slower BDC is confirmed by tracer-transport studies, indicating that the bias is not only related to the radiation budget, but also to transport (SPARC, 2022, Chap. 5). The SPARC report advises to use MERRA2 with caution in Brewer-Dobson circulation studies and for many BDC diagnostics, JRA-55 and ERA-Interim are more suitable (with limitations). ERA-Interim and JRA-55 are not used here because these do not reach high enough to capture the mesospheric chemistry of SF_6.

3 The BASCOE model

The model that is used in this work is the Chemistry Transport Model (CTM) of the Belgian Assimilation System for Chemical ObsErvations (BASCOE, Errera et al., 2008). This CTM is dedicated to stratospheric composition and includes around 60 chemical species. All species are advected by the flux-form semi-Lagrangian scheme (Lin and Rood, 1996) which conserves mass and preserves tracer-tracer correlations. Approximately 200 chemical reactions (gas phase, photolysis and heterogeneous) are taken into account, including a parametrization of Polar Stratospheric Cloud (PSC) microphysics (Errera et al., 2019). The gas-phase and photolysis reaction rates have been updated according to Burkholder et al. (2015). Chemical reactions are solved by a chemical kinetic preprocessor (KPP, Damian et al., 2002). Note that chemistry is not computed in the troposphere at altitudes below 400 hPa. The CTM is driven by meteorological analyses as described in Sect. 3.2. The following subsections first describe the update of the chemistry and then the preprocessing of the dynamical fields and details of the simulations.

3.1 Implementation of SF6 chemistry

SF_6 is inert in the stratosphere and is destroyed by attachment of electrons in the mesosphere producing a negative excited ion $(SF_6{}^-)^*$. SF_6 is partially recovered via stabilizing reactions, either directly via photodetachment of an electron, or by cycling the stabilized $SF_6{}^-$ back to SF_6 via several other reactions.

In order to model the distribution of SF_6, the BASCOE chemistry transport model has been updated with SF_6 chemistry. The reaction scheme used in this work was first described in Reddmann et al. (2001) and later used in the EMAC model (Loeffel et al., 2022). It is shown in Table 2. The main destruction mechanism for SF_6 is auto-attachment of electrons (R2). UV-photolysis (R1) is not used in BASCOE because the corresponding loss rate is negligible compared to the loss rate from electron auto-attachment (Totterdill et al., 2015). In addition to SF_6, the species $SF_6{}^-$ and $(SF_6{}^-)^*$ have been added to the

https://doi.org/10.5194/egusphere-2025-3597
Preprint. Discussion started: 13 August 2025

list of chemical compounds of BASCOE and the rate constants for the reactions were taken from Reddmann et al. (2001). The electron-attachment reaction produces an excited negative ion of SF_6, which in turn can stabilize and react with H, HCl, O3 or $h\nu$ to form SF_6 or other products. In order to implement these chemical reactions, the electron density and the computation of the photodetachment rate are needed. The electron density is parametrized taking as input the altitude, the latitude, the solar zenith angle, the O_2 column, the air density and the day of the year, using the same code as in EMAC (Reddmann et al., 2001; Loeffel et al., 2022). The relevant electrons are those from the D-region of the ionosphere (see Brasseur and Solomon (2005) Chap. 7 for a derivation of the electron density).

The photodetachment (R3) rate is calculated within the BASCOE model as a standard photolysis rate, via:

$$j_3(\theta) = \sum_i \sigma_{pd}(\lambda_i) F(\theta, \lambda_i, p) \Delta\lambda_i \tag{1}$$

Where σ_{pd} is the cross-section for photodetachment and F is the solar irradiance (actinic flux), dependent on the solar zenith angle θ, the wavelength λ_i and the pressure p. The cross-sections σ_{pd} are computed using a relation proposed by Datskos et al. (1995) for wavelengths below 337 nm and a constant cross-section of 2×10^{-18} for wavelengths above 337 nm, as proposed by Ingólfsson et al. (1994). The cross-sections as a function of wavelength and the photodetachment rate for one snapshot of BASCOE output as a function of latitude and corresponding solar zenith angle are shown in Fig. 1.

The loss rates α and the electron density computed in BASCOE were evaluated against published values. Figure 2a shows how the inverse loss rates from Reddmann et al. (2001) compare to the inverse loss rates in BASCOE on January 15, 2002. This plot also contains the loss rates from Totterdill et al. (2015), which agree well with the loss rates in BASCOE. The electron density in BASCOE is compared with other published electron fields in Fig. 2b. This shows that BASCOE follows the ionization profile from Reddmann et al. (2001). BASCOE electron density also agrees well with an observation taken from Brasseur and Solomon (2005), shown in Fig. 2b.

Table 2. Chemical scheme for SF_6

Reaction No.	Reaction	Reaction rate constant	Remarks
R1	$SF_6 + h\nu \rightarrow$ products		UV-photolysis
R2	$SF_6 + e^- \rightarrow (SF_6^-)^*$	$k_2 = 270 \times 10^{-9} cm^{-3} s^{-1}$	e^- auto-attachment
R3	$SF_6^- + h\nu \rightarrow SF_6 + e^-$	$j_3 \approx 0.02 s^{-1}$	photodetachment [1]
R4	$SF_6^- + H \rightarrow SF_5^+ + HF$	$k_4 = 0.21 \times 10^{-9} cm^{-3} s^{-1}$	
R5	$(SF_6^-)^* + M \rightarrow SF_6^-$	$k_5 = 0.19 \times 10^{-9} cm^{-3} s^{-1}$	stabilization
R6	$(SF_6^-)^* \rightarrow SF_6 + e^-$	$k_6 = 1 \times 10^6 s^{-1}$	auto-detachment [2]
R7	$SF_6^- + HCl \rightarrow$ products	$k_7 = 1.5 \times 10^{-9} cm^{-3} s^{-1}$	
R8	$SF_6^- + O_3 \rightarrow SF_6 + O_3^-$	$k_8 = 1.2 \times 10^{-9} cm^{-3} s^{-1}$	

[1] The value of j_3 is an indication of the final result of the photodetachment calculation.

[2] There is a typo in Table 1 of Reddmann et al. (2001) and the correct value was taken from its Sect. 2.2.

https://doi.org/10.5194/egusphere-2025-3597
Preprint. Discussion started: 13 August 2025

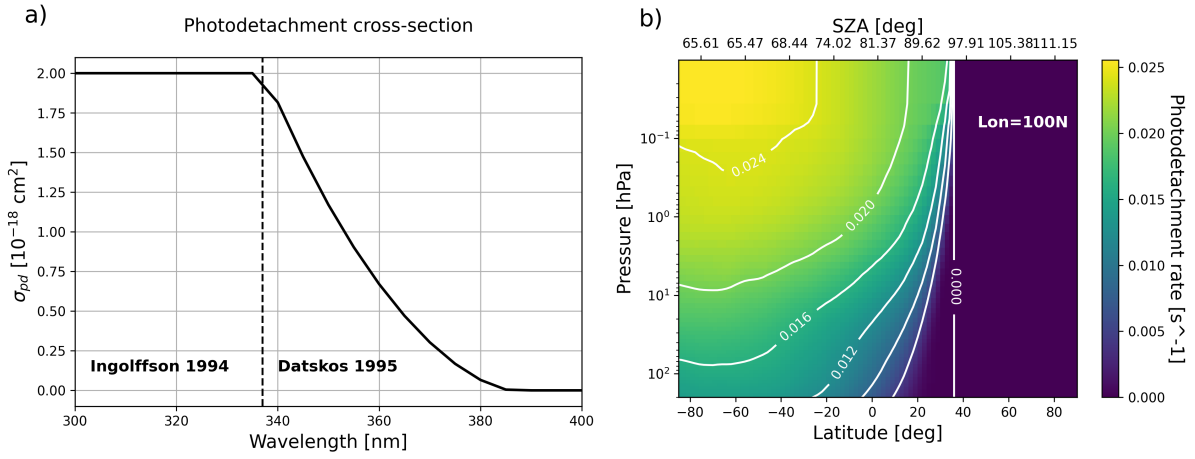

Figure 1. Left: photodetachment cross-sections computed from Ingólfsson et al. (1994) and Datskos et al. (1995). Right: photodetachment rate, computed in BASCOE, as a function of latitude with corresponding solar zenith angle (SZA) for a longitude of 100N on 2002-01-01 at 00:00.

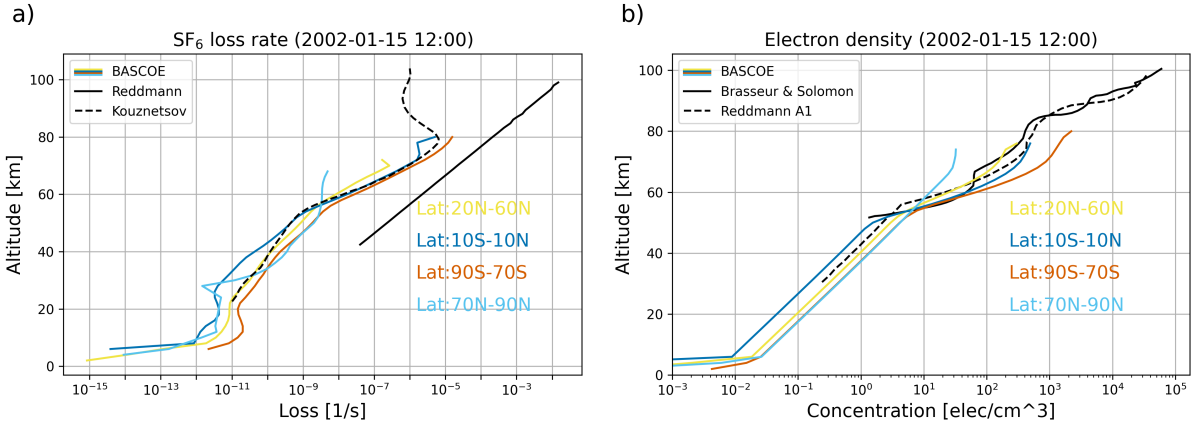

Figure 2. Left: comparison between the loss rates as shown in Reddmann et al. 2001 and Totterdill et al. (2015) with a BASCOE snapshot from 2002-01-15 (TRANS_M2_L49) in different latitude bands. Right: example profiles of the electron field of BASCOE, shown over 4 latitude bands, compared with the A and A1 profiles of Reddmann et al. (2001) and the electron density in Brasseur and Solomon (2005), Chap. 7, Fig.7.3.

3.2 Model simulations

This work presents three BASCOE CTM simulations of 25 years (1997-2023) driven by ERA5, MERRA2 and JRA-3Q, respectively, with a model time step of 30 minutes (see Table 3 summarizing the BASCOE simulations performed for this study). Reanalysis dynamical fields were reduced in resolution to match the BASCOE spatial grid using a mass-conserving preprocessor, following the approach in Chabrillat et al. (2018). This was done because simulating chemistry on the native

https://doi.org/10.5194/egusphere-2025-3597
Preprint. Discussion started: 13 August 2025

spatial grids of the reanalyses incurs a large computational cost and storage requirements which are not available on the BIRA-IASB computing system. The BASCOE simulations have been carried out with a horizontal resolution of 2°x2.5° latitude-longitude as in Chabrillat et al. (2018), which is sufficient to capture tropical and high-latitude mixing barriers (Strahan and Polansky, 2006). Similarly, the vertical resolution of the reanalyses has been reduced, since chemistry is not computed on most levels in the troposphere. The vertical regridding procedure is detailed in Appendix A. The native vertical resolution of the

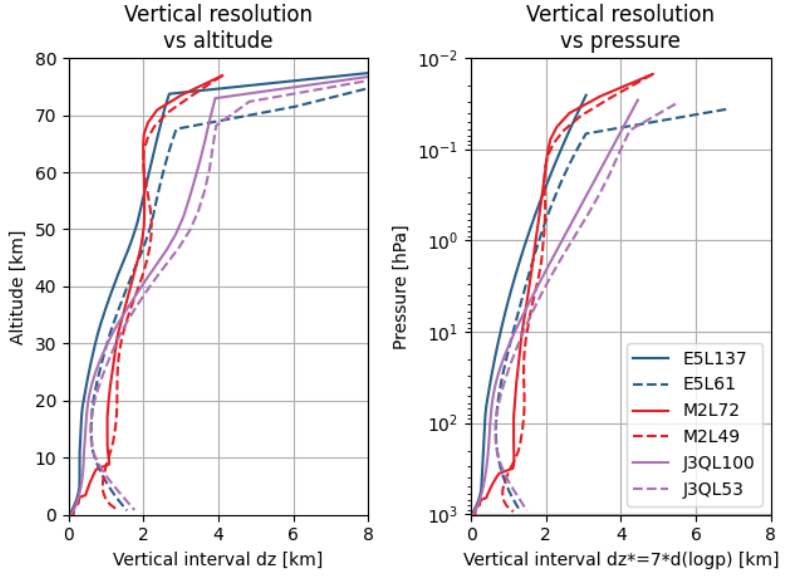

Figure 3. Vertical resolution of the different grids as a function of altitude (left) and the pressure (right). Blue, red and purple lines correspond, respectively, to ERA5, MERRA2 and JRA-3Q. Solid and dashed lines correspond, respectively, to native and reduced vertical resolution. Note that the line color of each reanalysis follows the A-RIP conventions, as in other figures.

reanalyses and those obtained by the vertical regridding are shown in Fig. 3. For ERA5, a grid with 61 levels was chosen, for MERRA2, 49 levels were chosen and finally the grid of JRA-3Q was reduced to 53 levels. From this figure it is clear that the resolution is now lower in the troposphere and, to a lesser extent, in the stratosphere and mesosphere.

To assess the transport on the reduced vertical grids, simulations of mean AoA using an idealized clock tracer were performed on both the native and the reduced grids. These simulations re-use meteorological fields from the same two years (1980-1981) of reanalysis data to drive the model in order to avoid the effect of climatological trends. Two years were chosen instead of one to capture the dynamical effects of the Quasi Biennial Oscillation (QBO), which is called a perpetual QBO set-up (Prignon, 2021). Each run lasts 20 years and the results are evaluated at the end of this period to avoid the spin-up of the model. The average of the model AoA from the last year of the perpetual QBO simulations is shown in Fig. 4. MERRA2 meteorology results in the highest AoA, followed by JRA-3Q, while ERA5 produces the lowest AoA. The simulations on the reduced and native grids are in good agreement, generally within 0.1 years. Slightly larger differences are found for MERRA2 (0.3 years) in the extra-tropics at 100 hPa, which is acceptable. This validates our choice for the reduced levels.

https://doi.org/10.5194/egusphere-2025-3597
Preprint. Discussion started: 13 August 2025

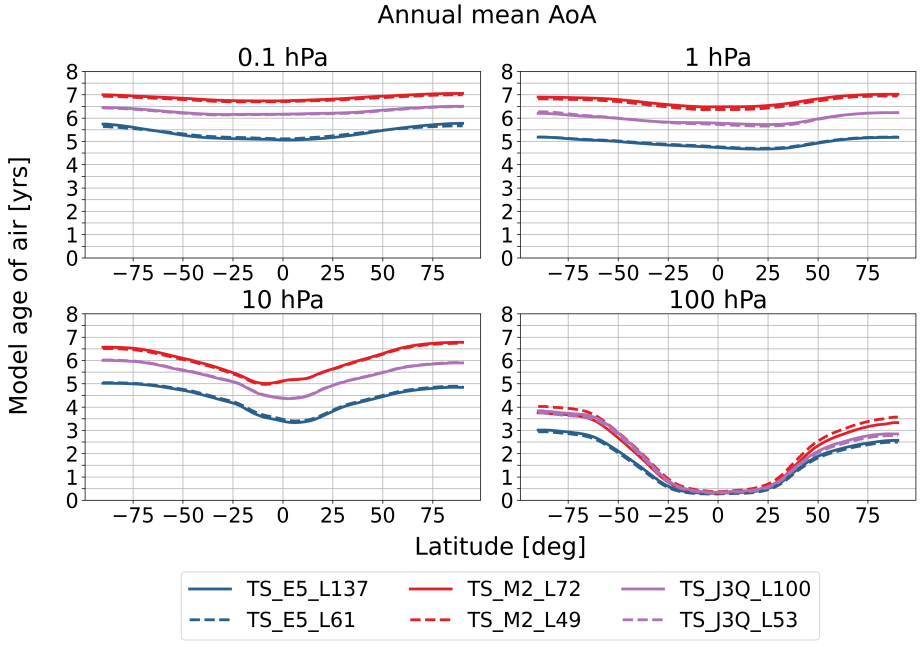

Figure 4. Model age of air from perpetual year simulations driven by ERA5, MERRA2 or JRA-3Q on their native (solid lines) and reduced (dashed lines) vertical grids, at different altitudes, averaged over the last year of the simulation.

Initial conditions were based on a BASCOE run driven by ERA5 (see Prignon et al., 2021), except for SF_6. For the latter, monthly zonal mean output from an EMAC model simulation was used to initialize the BASCOE simulations on 27-01-1997. This output comes from the specified dynamics simulation described in Loeffel et al. (2022), which has a model top at 0.01 hPa, spans the period 1980-2011 and is nudged to the ERA-Interim reanalysis. The lower boundary conditions for BASCOE were adapted from Meinshausen et al. (2017) for surface emissions from 1700 to 2014, and from Gidden et al. (2019) for emission projections under the shared socioeconomic pathway SSP2-4.5 beyond 2014.

At every time step of the simulation, BASCOE checks if observations are available for that time and interpolates the model output at the locations of the satellite observations. BASCOE was initially saved in the space of MIPAS V5 and ACE-FTS V4.1. Although newer data versions were later used, the model output was not reinterpolated to the new data locations, and therefore only subsets of the new data are used. This output in observation space is used to compute statistical differences between the model and the observations, presented in Sect. 5.1.

4 Global atmospheric lifetime

While evaluation of the model results with satellite observations is useful, it only provides validation for altitudes seen by the instruments. The global atmospheric lifetime of a gas, on the other hand, probes the entire atmosphere and can thus be

https://doi.org/10.5194/egusphere-2025-3597
Preprint. Discussion started: 13 August 2025

Table 3. BASCOE runs performed in this study

Label	Description	Simulated period	Chemistry
TS_E5_L137	Time slice simulation (perpetual QBO) driven by ERA5 on native grid	20 years	no
TS_E5_L61	Time slice simulation (perpetual QBO) driven by ERA5 on reduced grid with 61 levels	20 years	no
TS_M2_L72	Time slice simulation (perpetual QBO) driven by MERRA2 on native grid	20 years	no
TS_M2_L49	Time slice simulation (perpetual QBO) driven by MERRA2 on reduced grid with 49 levels	20 years	no
TS_J3Q_L100	Time slice simulation (perpetual QBO) driven by JRA-3Q on native grid with 100 levels	20 years	no
TS_J3Q_L53	Time slice simulation (perpetual QBO) driven by JRA-3Q on reduced grid with 53 levels	20 years	no
TRANS_E5_L61	Transient simulation driven by ERA5 on 61 levels	1997/01 - 2023/12	yes
TRANS_M2_L49	Transient simulation driven by MERRA2 on 49 levels	1997/01 - 2023/12	yes
TRANS_J3Q_L53	Transient simulation driven by JRA-3Q on 53 levels	1997/01 - 2023/12	yes

used as a diagnostic for the implementation of the SF_6 chemistry, as well as for the reanalysis data sets used in this work, by assessing the differences between the three simulations. The global atmospheric lifetime of species i is calculated at any time from BASCOE model output as the ratio between the global atmospheric burden and the global atmospheric loss rate:

$$\tau = \frac{\text{atmospheric burden}}{\text{atmospheric loss rate}} \tag{2}$$

which can be found in, for example, the 2013 SPARC report on lifetimes, chapter 2 (SPARC, 2013). This is the instantaneous lifetime and depends on the specific atmospheric conditions. The atmospheric burden is calculated as the total number of molecules of the species i, in other words $\int n_i dV = \int \chi_i n_{air} dV$ where n_i is the number density of species i, n_{air} is the air density, χ_i is the volume mixing ratio of species i, and the integral runs over all grid cells of the model with volume dV. The atmospheric loss rate is a similar integral, but it includes the net chemical loss frequencies α_i, so that the integral is given by $\int \alpha_i n_i dV$. The loss rate of species i is written as:

$$\frac{dn_i}{dt} = -\alpha_i n_i \tag{3}$$

with

$$\alpha_i = L_i - \frac{P_i}{n_i} \tag{4}$$

where P_i is the local production of species i in molec/cm^3/s, and L_i is the local loss in 1/s. These quantities P_i and L_i are computed by the chemical kinetic preprocessor and stored in the output files of BASCOE. Using equations (3) and (4) the global lifetime can be computed from every snapshot of model output. To smooth out seasonal variability, the lifetime is averaged over the period 2002-2012.

https://doi.org/10.5194/egusphere-2025-3597
Preprint. Discussion started: 13 August 2025

For CH_4 and HCFC-22, the reaction with OH in the troposphere is the most important destruction process. Since BASCOE does not compute chemistry in the lower troposphere, only the stratospheric lifetime (and not the global lifetime) of these species is computed, i.e. integrating the loss rates above 200 hPa in the tropics (between $\pm$ 30°) and above 400 hPa at other latitudes.

5 Results and discussion

5.1 Comparison with independent observations

The results of the BASCOE simulations have been compared to MIPAS and ACE-FTS satellite observations. The normalized mean bias (NMB) between the BASCOE simulation and the satellite profiles, the associated standard deviation (STD) and their correlations (Correl) are shown in Fig. 5 in the tropics and in Fig. 6 in the southern high latitudes (60S-90S). These statistics are computed over the period Jan. 2005 - Apr. 2012 for MIPAS and Feb. 2004 - Apr. 2012 for ACE-FTS. For SF_6, the agreement between the BASCOE model runs and the two instruments is within the instrument differences (see Table 1) and the bias is mostly limited to $\pm$ 10%.

For N_2O and CH_4, the comparisons are within the range of uncertainty between MIPAS and ACE-FTS below 10 hPa and increase at high altitude where their chemical losses are more pronounced. For CFC-11 in the lower stratosphere, the bias is also in agreement with the instrumental uncertainties and for HCFC-22 the bias is in agreement with the instrumental bias of around 14% at 25km ($\sim$ 25 hPa) found in Kolonjari et al. (2024). For CFC-12 the biases are somewhat larger than expected, showing biases of more than 20% above 30 hPa, which is larger than the 10% instrumental bias between MIPAS and ACE-FTS SPARC (2017). An explicit comparison between MIPAS and ACE-FTS is difficult here due to sampling effects. For SF_6 the simulation driven by MERRA2 has a lower bias with respect to MIPAS than the simulations driven by ERA5 or JRA-3Q. For all species, the standard deviation is relatively small (<10%) at altitudes where their photochemical loss is small and increase at higher levels. The correlation is also better in the lower stratosphere (>0.8) and decreases at higher levels.

Figures 7 and 8 show time series of the normalized mean bias (NMB) and the normalized standard deviation (NSD) at different levels for SF_6. The time series in Fig. 7 emphasizes the temporal stability of the results in the tropics and at mid to low altitude. The bias is relatively stable and limited mostly to 10% in the tropics. At the Poles, the bias shows seasonal variability with an amplitude around 20% at 1 hPa. The seasonality of the bias is also reflected in the standard deviation.

This oscillating pattern is found for all trace gases in this study (see the supplement where similar figures for the other long-lived tracers are available). The standard deviation is around 10-15% in the tropical lower stratosphere and increases towards the Poles.

The standard deviation shows a slight decreasing trend.This is due to the fact that the surface emissions of SF_6 significantly increase over the course of the shown period, thus reducing the relative noise in the observations. A similar pattern is found for HCFC-22 for the same reason (see Fig. S16).

https://doi.org/10.5194/egusphere-2025-3597
Preprint. Discussion started: 13 August 2025

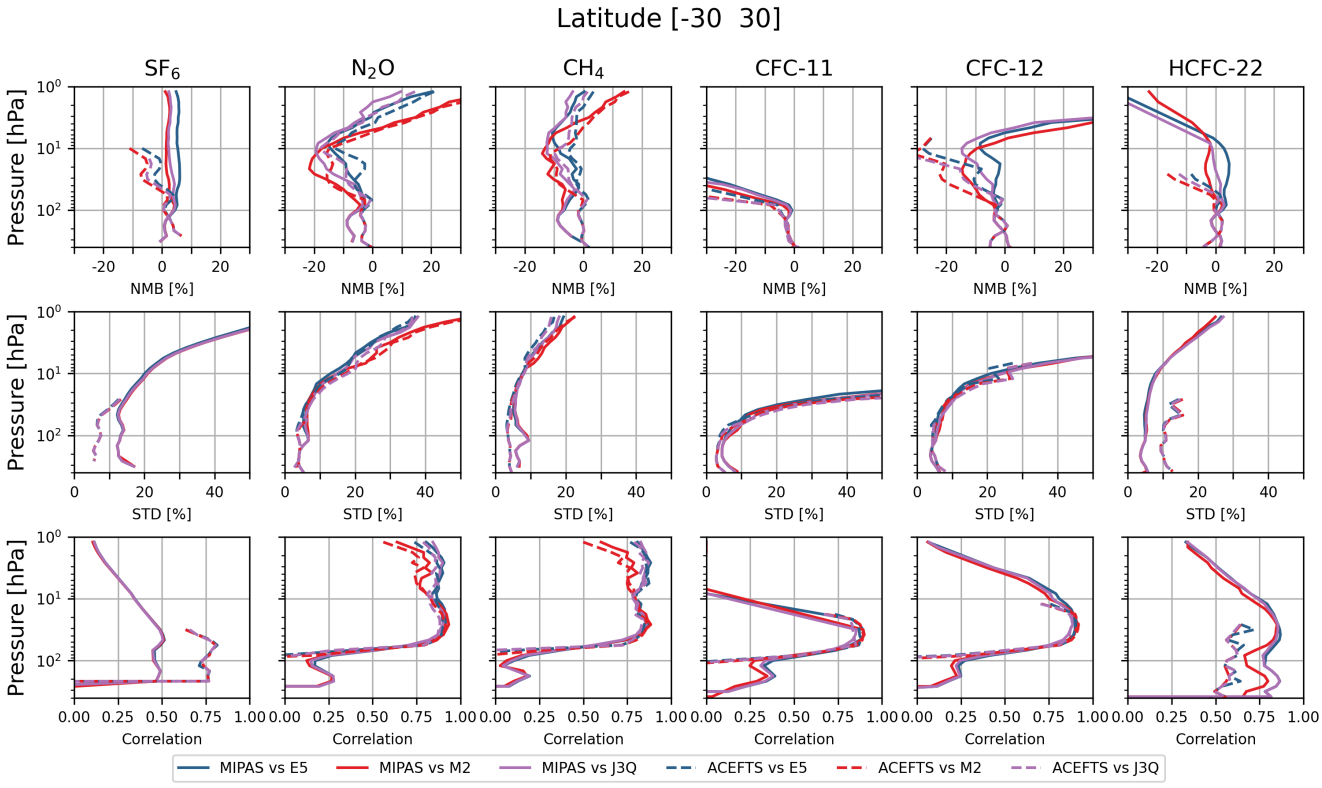

Figure 5. Normalized mean bias (NMB), standard deviation (STD) and correlation (Correl) of all six long-lived species over the tropics. Data is cut off at 1hPa because there are insufficient observations above this pressure level.

5.2 Global atmospheric lifetime

Figure 9 shows the global atmospheric lifetimes from the three BASCOE runs, averaged over 2002-2012. The error bars indicate the 1σ variability of the lifetime time series from BASCOE over the considered period 2002-2012. The results are compared with lifetimes found in the literature, shown as error bars here to indicate the possible range of values with a marker at the best value if provided in the source paper. These reference values are not specifically for the period 2002-2012. The error bar on the value from Loeffel et al. (2022) could be reduced to 1900 - 2100 for this period. The lifetimes of the long-lived species N_2O, CH_4, CFC-11, CFC-12 and HCFC-22 (see Fig. 9a) show good agreement with results from the literature (SPARC, 2013; Volk et al., 1997; Prather et al., 2023; Fleming et al., 2015; Minschwaner et al., 2013; Moore and Remedios, 2008; Avallone and Prather, 1997; Kanakidou et al., 1995; Spivakovsky et al., 2000) and between the reanalyses. Since CH_4 and HCFC-22 have significant sinks in the troposphere, and since BASCOE is not designed for tropospheric chemistry, the stratospheric lifetime of these species has been computed and compared with stratospheric lifetimes from the literature. The consistency between the three different simulations for the 5 species mentioned above and the agreement with the literature creates confidence in our

https://doi.org/10.5194/egusphere-2025-3597
Preprint. Discussion started: 13 August 2025

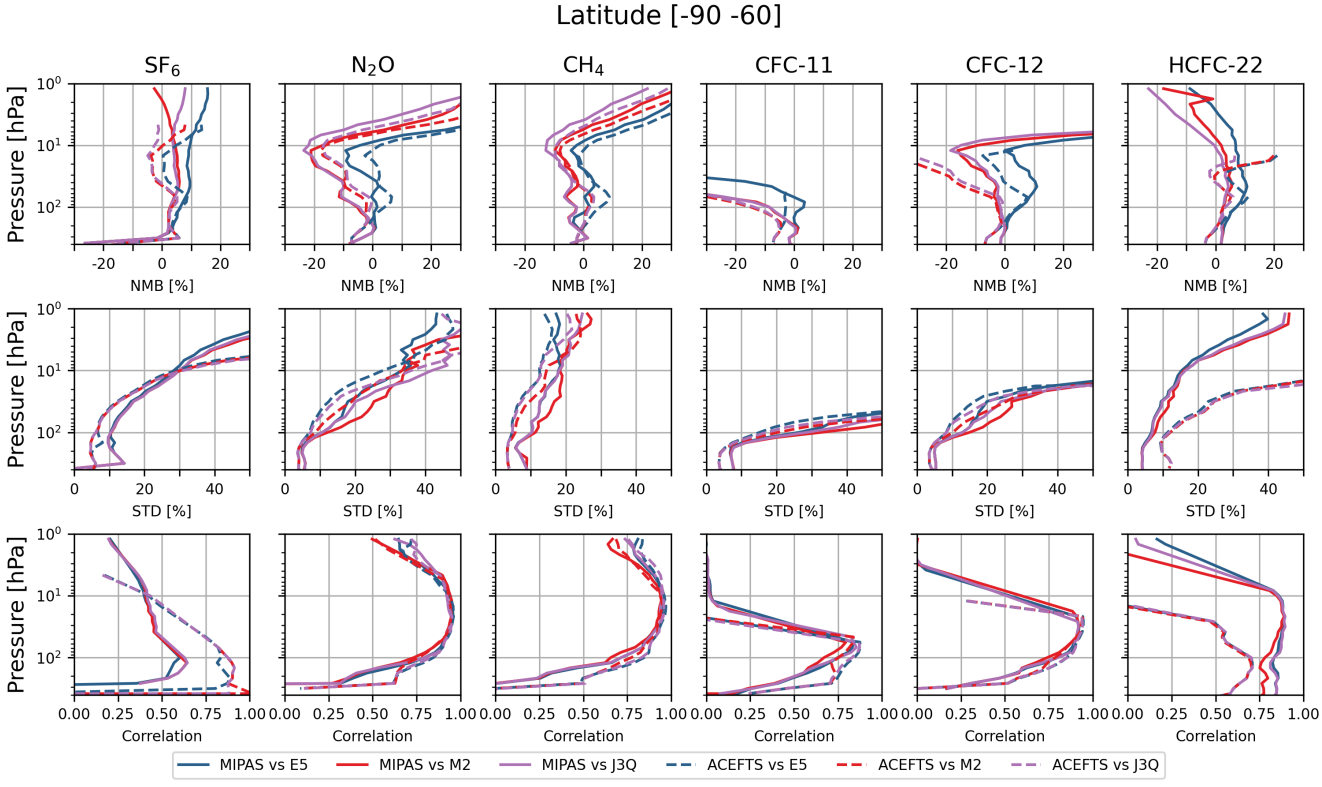

Figure 6. Same as Fig. 5, but for the South Pole.

lifetime computation. The lifetimes of all six species are summarized in Table 4. The global atmospheric lifetime of SF_6 has been computed in several studies over the last 30 years (Krey et al., 1977; Ravishankara et al., 1993; Ko et al., 1993; Morris et al., 1995; Harnisch et al., 1999; Reddmann et al., 2001; Patra et al., 2009; Ray et al., 2017; Kovács et al., 2017; Kouznetsov et al., 2020; Loeffel et al., 2022). This body of work is summarized in Fig. 9b. The black bars are organized (from left to right) from the oldest to the most recent publication. The values show a large spread. Ravishankara et al. (1993) proposed a value of 3200 years from model computations, but noted that taking into account electron attachment could significantly reduce the lifetime, hence the lower limit of 580 years. In later works, the importance of the mesospheric sink is generally recognised. The average lifetime of SF_6 in BASCOE over the period 2002-2012 is 2646 $\pm$ 532 years with an ERA5 driven run, 1909 $\pm$ 182 years with a MERRA2 driven run and 2145 $\pm$ 459 years with a JRA-3Q driven run as shown in color in panel b. The BASCOE results show good agreement with the result from the transient reference simulation (REF) and the simulation nudged to ERA-Interim in Loeffel et al. (2022), using the global chemistry climate model EMAC. This is especially true for the simulation driven by JRA-3Q. The lifetime from the simulation driven by MERRA2 is similar to the lifetime from the time slice simulation (TS2000) in Loeffel et al. (2022), which uses fixed climate conditions from the year 2000. The lifetime derived

https://doi.org/10.5194/egusphere-2025-3597
Preprint. Discussion started: 13 August 2025

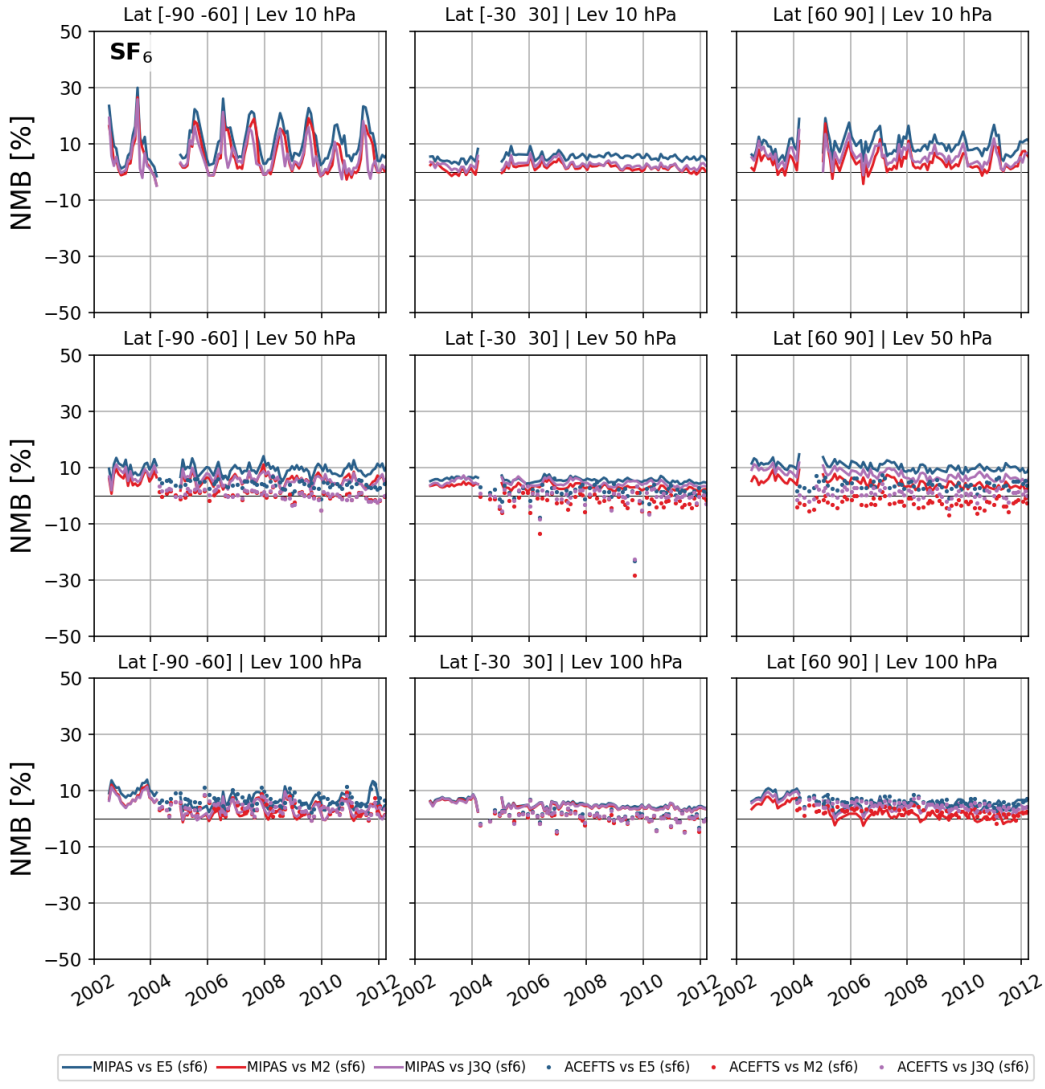

Figure 7. Timeseries of the normalized mean bias of SF_6 volume mixing ratios with respect to MIPAS and ACE-FTS for three latitude bands and three pressure levels.

from the ERA5-driven simulation is closer to the their CSS simulation, which uses the same climate conditions as the transient reference simulation, but sets the concentrations of the SF_6 reactant species to 1950 levels.

For N_2O, CH_4, CFC-11, CFC-12 and HCFC-22, the lifetimes derived from the three different simulations are closely aligned (see Fig. 9a), indicating that there is little sensitivity to meteorology for these species, possibly due to good agreement between

https://doi.org/10.5194/egusphere-2025-3597
Preprint. Discussion started: 13 August 2025

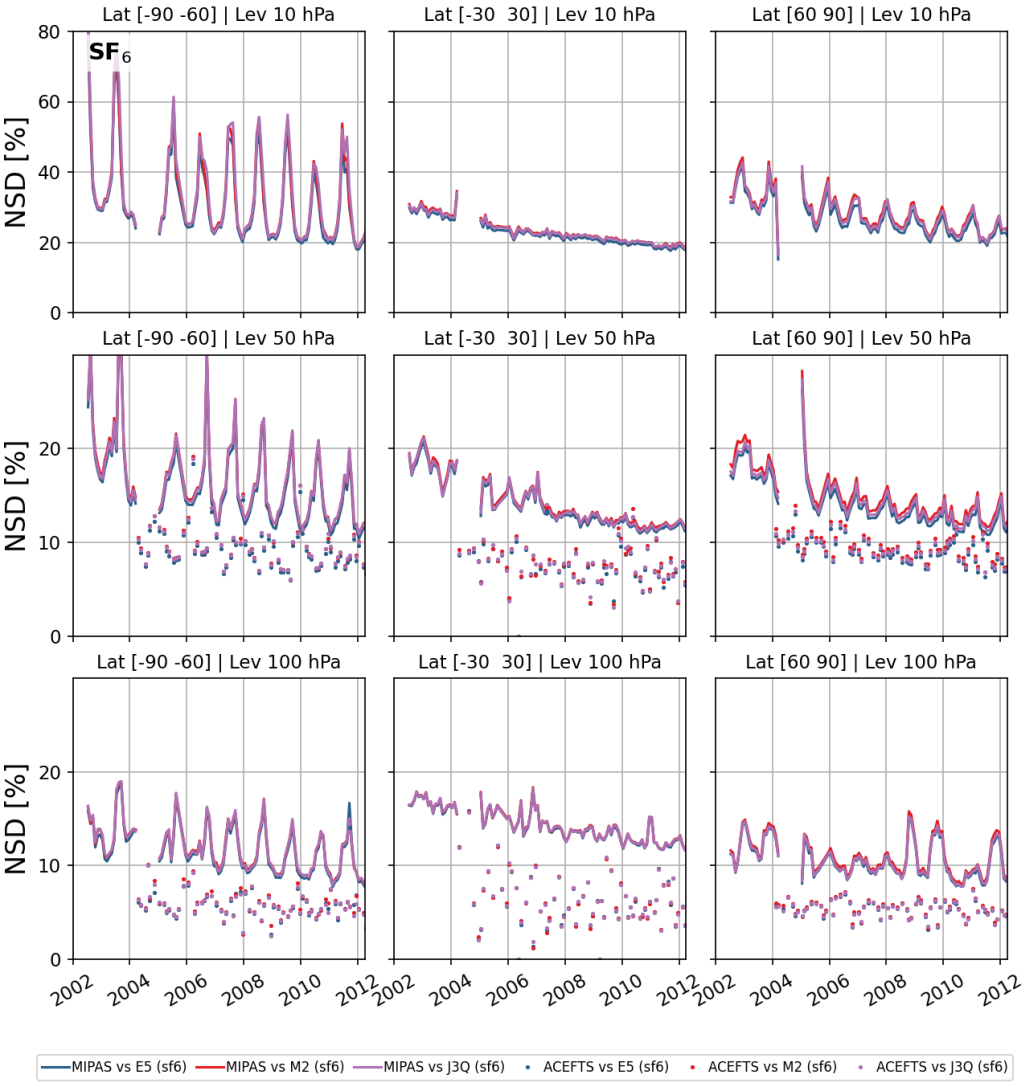

Figure 8. Timeseries of the standard deviation of SF_6 for three latitude bands and three pressure levels.

the reanalyses at altitudes where the species are destroyed. However, CTM-E5 consistently produces a slightly lower lifetime than CTM-M2, CTM-J3Q being often in between. For SF_6 there are relatively large differences between the three values. This could be explained by the lack of stratospheric and mesospheric observations to constrain the reanalyses in the region where SF_6 chemistry is important, as well as the differences in the sponge layers between the three reanalyses. Also, contrary to the 5 other species, SF_6 lifetime from CTM-E5 is significantly longer than the lifetime from CTM-J3Q and CTM-M2. We

https://doi.org/10.5194/egusphere-2025-3597
Preprint. Discussion started: 13 August 2025

hypothesize that SF_6 spends less time in the mesosphere due to the faster circulation with ERA5 and is therefore able to return to the stratosphere via recirculation, resulting in higher volume mixing ratios in the stratosphere and thus a longer lifetime.

The time series of the lifetime of all six species and the tropical temperature at 1 hPa are shown in Fig. 10. There is an increasing trend in the lifetime of CH_4, consistent with predictions from Li et al. (2022), but not for the other species, while Prather and Holmes (2013) found a decreasing trend of N_2O lifetimes. There is no clear trend in the SF_6 lifetime, in contrast to the increasing trend in the reference simulation and the projected simulation from Loeffel et al. (2022). In the time series, a semi-annual oscillation (SAO, Reed, 1965) is observed. The SAO is more apparent and more regular for CH_4 and HCFC-22 than for CFC-11, CFC-12 and N_2O. SAO's in the winds and temperature have been previously observed near the stratopause around 1 hPa and near the mesopause at around 0.01 hPa. The SAO in the stratosphere is linked to the passage of the Sun across the equator that happens twice per year and the absorption of solar UV by ozone in the stratosphere. The origin of the mesospheric SAO is not well understood, but there is thought to be a lag between the stratospheric and the mesospheric SAO, and that the mesospheric SAO is related to gravity and Kelvin waves. The temperature is plotted in the tropics at 1 hPa, the region where the SAO is the strongest (Shangguan and Wang, 2023). While similar patterns are observed between the temperature at 1 hPa in the tropics and the time series of the lifetime, the link between both quantities is not clear. For SF_6, the amplitude of the seasonal variation of the lifetime is larger for CTM-E5 than for the two other simulations. This could be related to the stronger seasonal cycle in the total tropical upwelling of ERA5 with respect to MERRA2 (SPARC, 2022, Chap. 5).

Table 4. Average lifetime (years) of six long-lived trace gases from the different BASCOE simulations for the period 2002-2012. For CH_4 and HCFC-22, stratospheric lifetime is shown, while global atmospheric lifetime is shown for the other species.

Experiment	N_2O	CH_4	CFC-11	CFC-12	HCFC-22	SF_6
TRANS_E5_L61	130 ± 10	144 ± 7	52 ± 5	108 ± 9	198 ± 11	2646 ± 532
TRANS_M2_L49	135 ± 14	147 ± 8	59 ± 7	115 ± 14	204 ± 12	1909 ± 182
TRANS_J3Q_L53	135 ± 11	142 ± 7	56 ± 5	114 ± 10	195 ± 11	2147 ± 459

https://doi.org/10.5194/egusphere-2025-3597
Preprint. Discussion started: 13 August 2025

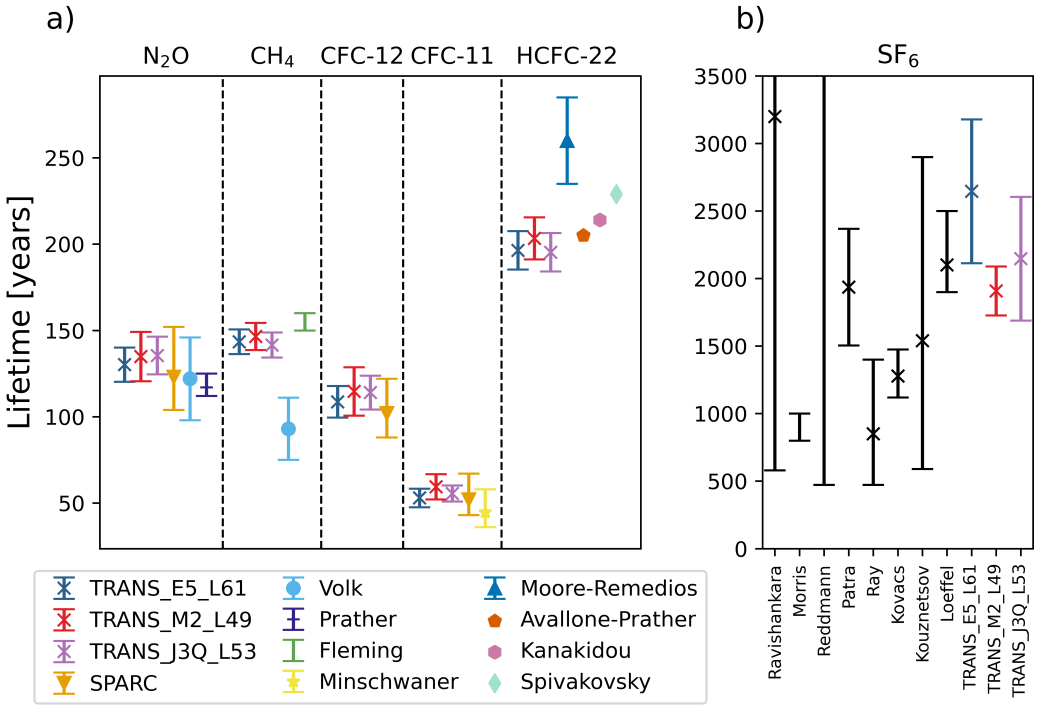

Figure 9. Lifetime of atmospheric trace gases averaged over 2002-2012. The SF_6 lifetimes from the literature are shown as error bars without marker point if only a range was given, or as an error bar with a marker at the most likely lifetime value, or as a single point if only one value was given. The lifetimes for CH_4 and HCFC-22 are integrated only over stratospheric levels (see methods)

https://doi.org/10.5194/egusphere-2025-3597
Preprint. Discussion started: 13 August 2025

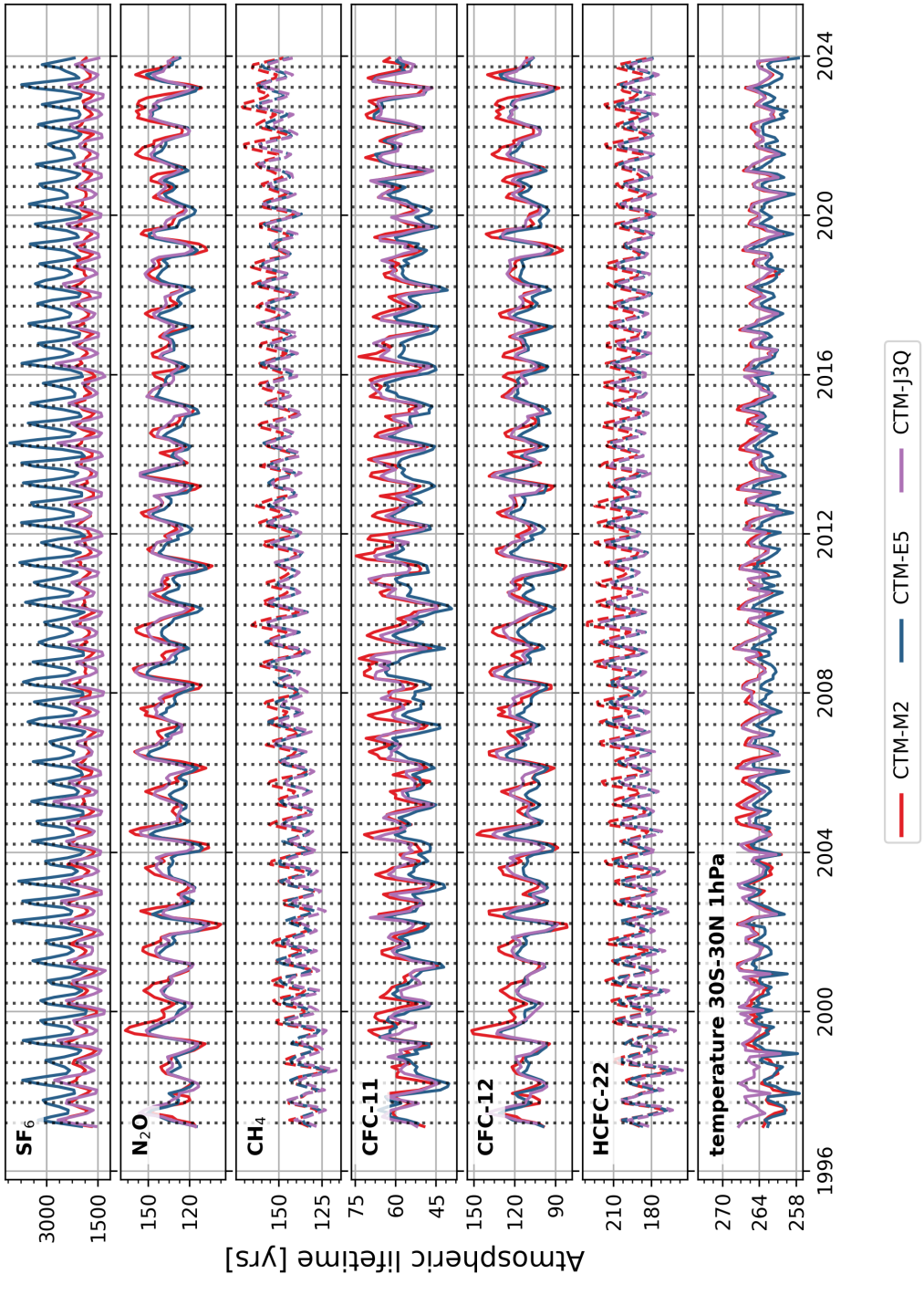

Figure 10. Global atmospheric lifetime (solid lines) or stratospheric lifetime (dashed lines) of different species computed from BASCOE simulation drived by ERA5 (blue lines), MERRA2 (red lines) and JRA-3Q (purple lines).

https://doi.org/10.5194/egusphere-2025-3597
Preprint. Discussion started: 13 August 2025

6 Conclusions

The chemistry of SF_6 has been implemented in the Belgian Assimilation System for Chemical ObsErvations (BASCOE). Three model simulations have been carried out, driven by three recent meteorological reanalyses (ERA5, MERRA2 and JRA-3Q) that include the mesosphere where SF_6 is destroyed via auto-attachment with electrons. These simulations show a relatively good agreement with MIPAS and ACE-FTS satellite observations in the middle and low stratosphere with biases generally within $\pm 10\%$ for SF_6 volume mixing ratios and within the estimated instrumental uncertainties for all six species below 10 hPa. For SF_6, the simulation driven by MERRA2 has a slightly lower bias with respect to MIPAS than those driven by ERA5 and JRA-3Q. The global atmospheric lifetime of SF_6 was computed and compared with published results to further assess the impact of the choice of meteorology in the mesosphere where satellite observations provide little information. The lifetime was also computed for the other long-lived species. The computed lifetime of SF_6 - 2646 $\pm$ 532 years (ERA5), 1909 $\pm$ 182 years (MERRA2) and 2147 $\pm$ 459 years (JRA-3Q) - is consistent with recent results by Loeffel et al. (2022), but demonstrates the sensitivity of SF_6-derived transport diagnostics to the underlying meteorological data. For the other trace gases, the lifetimes from the three simulations are in good agreement between themselves and with published results, which confirms the validity of our lifetime calculation. A semi-annual oscillation is observed in the time evolution of the lifetimes of all six species, which exhibits similar patterns as tropical stratospheric temperature variations. A follow-up study is necessary to further investigate the differences in stratospheric transport among the three reanalyses in order to explain the differences in seasonal variation observed in the lifetime. With this model update, BASCOE is ready to perform further transport studies based on SF_6 diagnostics.

Appendix A: Computation of the reduced grids

This appendix describes the procedure to construct a vertical grid with reduced resolution for the reanalyses. The reanalyses used in this work are defined on a hybrid sigma-pressure grid. The pressure at level interface $p_{mid}(i)$ is defined by the model level parameters $A_p(i)$ and $B_p(i)$ as follows:

$$p_{mid}(i) = Ap(i) + Bp(i) \cdot p_{surf} \tag{A1}$$

with p_{surf} being the surface pressure and $i = 1, \text{nlev}$ is the level index and nlev is the number of model levels. The reduced grids are obtained as follows, see also the illustration in Fig. A1:

- Step 1: For several altitudes between 5 and 90 km, values of the desired vertical resolution dz were provided, hereby aiming to stay close to the native resolution in the upper levels and reducing the resolution in the troposphere.
- Step 2: These proposed altitude-resolution points were then fitted with a polynomial.
- Step 3: Starting from the surface, the vertical resolution at the lowest level is calculated using this polynomial, and this defines the altitude of the lowest level. Then level i+1 was calculated by incrementing level i with the vertical interval dz from the polynomial at level i, ensuring that the top levels correspond to the top levels of the reanalysis.

https://doi.org/10.5194/egusphere-2025-3597
Preprint. Discussion started: 13 August 2025

– Step 4: Then the native A_p and B_p are interpolated to the new vertical grid using a log-pressure approximation for the altitude. From the new A_p and B_p coefficients, the sigma-pressure levels were computed.

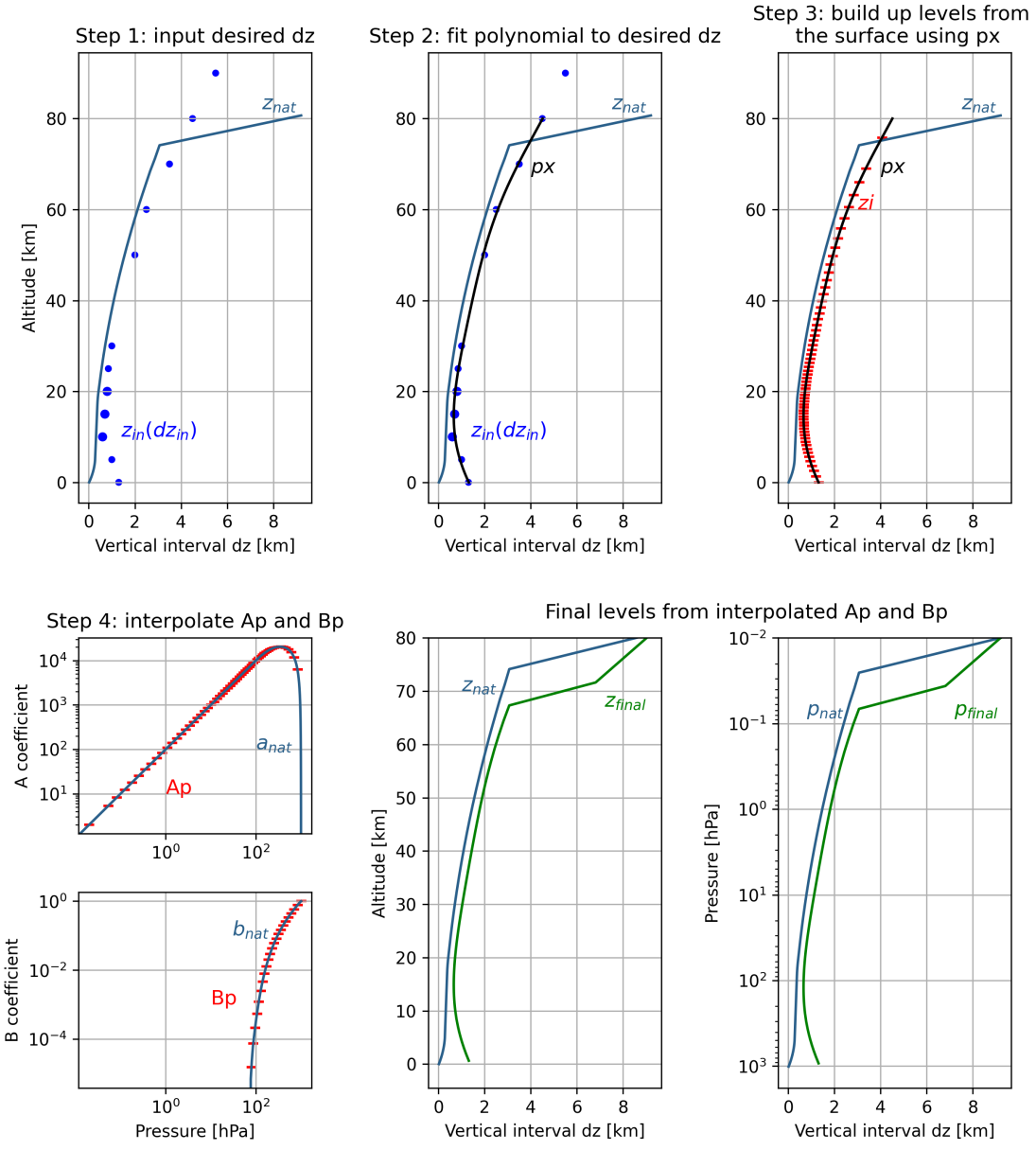

Figure A1. Workflow to construct a new grid for the reanalyses with desired vertical resolution (see text for details).

https://doi.org/10.5194/egusphere-2025-3597
Preprint. Discussion started: 13 August 2025

Code availability. The BASCOE code is available upon request.

Data availability. The MIPAS data is available at https://www.imk-asf.kit.edu/english/308.php. The ACE-FTS data is available at https://uwaterloo.ca/atmospheric-chemistry-experiment/. Monthly zonal mean BASCOE output is temporarily available to reviewers at https://webdav.aeronomie.be/guest/bascoe/Sarahv/BASCOE_data/. Upon acceptance, the data will be deposited in a public repository and the link will be provided in the final version of the article.

Author contributions. SV executed the implementation of the chemistry, carried out the simulations and visualized and interpreted the results. QE and EM provided the idea for the study, supervised the work and contributed to the interpretation of the results and revising of the manuscript. EM is senior research associate with F.R.S.-FNRS". SC and MOB helped with the interpretation of the results and provided feedback on the manuscript. TR provided support in the implementation of SF_6 chemistry in BASCOE and provided feedback on preliminary results. GS provided support in the use of MIPAS data sets. RE provided the EMAC data set and provided feedback on preliminary results.

Competing interests. At least one of the authors is a member of the editorial board of Atmospheric Chemistry and Physics.

https://doi.org/10.5194/egusphere-2025-3597
Preprint. Discussion started: 13 August 2025

References

Austin, J. and Li, F.: On the relationship between the strength of the Brewer-Dobson circulation and the age of stratospheric air, Geophysical research letters, 33, https://doi.org/10.1029/2006GL026867, 2006.

Avallone, L. M. and Prather, M. J.: Tracer-tracer correlations: Three-dimensional model simulations and comparisons to observations, Journal of Geophysical Research: Atmospheres, 102, 19 233–19 246, https://doi.org/10.1029/97JD01123, 1997.

Bernath, P. F., McElroy, C. T., Abrams, M., Boone, C. D., Butler, M., Camy-Peyret, C., Carleer, M., Clerbaux, C., Coheur, P.-F., Colin, R., et al.: Atmospheric chemistry experiment (ACE): mission overview, Geophysical research letters, 32, https://doi.org/10.1029/2005GL022386, 2005.

Brasseur, G. P. and Solomon, S.: Aeronomy of the Middle Atmosphere, 2005.

Brewer, A.: Evidence for a world circulation provided by the measurements of helium and water vapour distribution in the stratosphere, Quart. J. Roy. Meteorol. Soc., 75, 351–363, https://doi.org/10.1002/qj.49707532603, 1949.

Burkholder, J., Sander, S., Abbatt, J., Barker, J., Huie, R., Kolb, C., Kurylo, M., Orkin, V., Wilmouth, D., and Wine, P.: Chemical kinetics and photochemical data for use in atmospheric studies: evaluation number 18, Tech. rep., Pasadena, CA: Jet Propulsion Laboratory, National Aeronautics and Space . . . , 2015.

Butchart, N.: The Brewer-Dobson circulation, Rev. Geophys., 52, 157–184, https://doi.org/10.1002/2013RG000448, 2014.

Butchart, N. and Scaife, A. A.: Removal of chlorofluorocarbons by increased mass exchange between the stratosphere and troposphere in a changing climate, Nature, 410, 799–802, https://doi.org/10.1038/35071047, 2001.

Butchart, N., Scaife, A. A., Bourqui, M., Grandpré, J., Hare, S. H., Kettleborough, J., Langematz, U., Manzini, E., Sassi, F., Shibata, K., Shindell, D., and Sigmond, M.: Simulations of anthropogenic change in the strength of the Brewer-Dobson circulation, Clim. Dynam., 27, 727–741, https://doi.org/10.1007/s00382-006-0162-4, 2006.

Calvo, N. and Garcia, R. R.: Wave forcing of the tropical upwelling in the lower stratosphere under increasing concentrations of greenhouse gases, J. Atmos. Sci., 66, 3184–3196, https://doi.org/10.1175/2009JAS3085.1, 2009.

Chabrillat, S., Vigouroux, C., Christophe, Y., Engel, A., Errera, Q., Minganti, D., Monge-Sanz, B. M., Segers, A., and Mahieu, E.: Comparison of mean age of air in five reanalyses using the BASCOE transport model, Atmos. Chem. Phys., 18, 14 715–14 735, https://doi.org/10.5194/acp-18-14715-2018, 2018.

Damian, V., Sandu, A., Damian, M., Potra, F., and Carmichael, G. R.: The kinetic preprocessor KPP-a software environment for solving chemical kinetics, Comput. Chem. Eng., 26, 1567–1579, https://doi.org/10.1016/S0098-1354(02)00128-X, 2002.

Datskos, P. G., Carter, J. G., and Christophorou, L. G.: Photodetachment of SF6, Chem. Phys. Lett., 239, 38–43, https://doi.org/10.1016/0009-2614(95)00417-3, 1995.

Dietmüller, S., Eichinger, R., Garny, H., Birner, T., Boenisch, H., Pitari, G., Mancini, E., Visioni, D., Stenke, A., Revell, L., Rozanov, E., Plummer, D. A., Scinocca, J., Jöckel, P., Oman, L., Deushi, M., Kiyotaka, S., Kinnison, D. E., Garcia, R., Morgenstern, O., Zeng, G., Stone, K. A., and Schofield, R.: Quantifying the effect of mixing on the mean age of air in CCMVal-2 and CCMI-1 models, 18, 6699–6720, https://doi.org/10.5194/acp-18-6699-2018.

Dobson, G. M. B.: Origin and distribution of the polyatomic molecules in the atmosphere, Proceedings of the Royal Society of London. Series A. Mathematical and Physical Sciences, 236, 187–193, https://doi.org/10.1098/rspa.1956.0127, 1956.

Dobson, G. M. B., Kimball, H., and Kidson, E.: Observations of the amount of ozone in the earth's atmosphere, and its relation to other geophysical conditions.—Part IV, Proc. R. Soc. London A., 129, 411–433, https://doi.org/10.1098/rspa.1930.0165, 1930.

https://doi.org/10.5194/egusphere-2025-3597
Preprint. Discussion started: 13 August 2025

Eichinger, R., Dietmüller, S., Garny, H., Šácha, P., Birner, T., Bönisch, H., Pitari, G., Visioni, D., Stenke, A., Rozanov, E., Revell, L., Plummer, D. A., Jöckel, P., Oman, L., Deushi, M., Kinnison, D. E., Garcia, R., Morgenstern, O., Zeng, G., Stone, K. A., and Schofield, R.: The influence of mixing on the stratospheric age of air changes in the 21st century, 19, 921–940, https://doi.org/10.5194/acp-19-921-2019.

Errera, Q., Daerden, F., Chabrillat, S., Lambert, J. C., Lahoz, W. A., Viscardy, S., Bonjean, S., and Fonteyn, D.: Atmospheric Chemistry and Physics 4D-Var assimilation of MIPAS chemical observations: ozone and nitrogen dioxide analyses, https://doi.org/10.5194/acp-8-6169-2008, 2008.

Errera, Q., Chabrillat, S., Christophe, Y., Debosscher, J., Hubert, D., Lahoz, W., Santee, M. L., Shiotani, M., Skachko, S., von Clarmann, T., et al.: Reanalysis of Aura MLS chemical observations, Atmos. Chem. Phys., 19, 13 647–13 679, https://doi.org/10.5194/acp-19-13647-2019, 2019.

Fischer, H., Birk, M., Blom, C., Carli, B., Carlotti, M., Von Clarmann, T., Delbouille, L., Dudhia, A., Ehhalt, D., Endemann, M., et al.: MIPAS: an instrument for atmospheric and climate research, Atmos. Chem. Phys., 8, 2151–2188, https://doi.org/10.5194/acp-8-2151-2008, 2008.

Fleming, E. L., George, C., Heard, D. E., Jackman, C. H., Kurylo, M. J., Mellouki, W., Orkin, V. L., Swartz, W. H., Wallington, T. J., Wine, P. H., and Burkholder, J. B.: The impact of current CH4 and N2O atmospheric loss process uncertainties on calculated ozone abundances and trends, J. Geophys. Res., 120, 5267–5293, https://doi.org/10.1002/2014JD022067, 2015.

Garcia, R. R. and Randel, W. J.: Acceleration of the brewer-dobson circulation due to increases in greenhouse gases, J. Atmos. Sci., 65, 2731–2739, https://doi.org/10.1175/2008JAS2712.1, 2008.

Garny, H., Birner, T., Bönisch, H., and Bunzel, F.: The effects of mixing on age of air, 119, 7015–7034, https://doi.org/10.1002/2013jd021417.

Garny, H., Ploeger, F., Abalos, M., Boenisch, H., Castillo, A., von Clarmann, T., Diallo, M., Engel, A., Laube, J., Linz, M., et al.: Age of stratospheric air: Progress on processes, observations, and long-term trends, Rev. Geophys., 62, e2023RG000 832, https://doi.org/10.1029/2023RG000832, 2024.

Gelaro, R., McCarty, W., Suárez, M. J., Todling, R., Molod, A., Takacs, L., Randles, C. A., Darmenov, A., Bosilovich, M. G., Reichle, R., et al.: The modern-era retrospective analysis for research and applications, version 2 (MERRA-2), Journal of climate, 30, 5419–5454, https://doi.org/10.1175/JCLI-D-16-0758.1, 2017.

Gidden, M. J., Riahi, K., Smith, S. J., Fujimori, S., Luderer, G., Kriegler, E., Vuuren, D. P. V., Berg, M. V. D., Feng, L., Klein, D., Calvin, K., Doelman, J. C., Frank, S., Fricko, O., Harmsen, M., Hasegawa, T., Havlik, P., Hilaire, J., Hoesly, R., Horing, J., Popp, A., Stehfest, E., and Takahashi, K.: Global emissions pathways under different socioeconomic scenarios for use in CMIP6: A dataset of harmonized emissions trajectories through the end of the century, Geosci. Model Dev., 12, 1443–1475, https://doi.org/10.5194/gmd-12-1443-2019, 2019.

Hall, T. M. and Plumb, R. A.: Age as a diagnostic of stratospheric transport, J. Geophys. Res., 99, 1059–1070, https://doi.org/10.1029/93JD03192, 1994.

Harnisch, J., Borchers, R., Fabian, P., and Maiss, M.: Cf4 and the age of mesospheric and polar vortex air, Geophys. Res. Lett., 26, 295–298, https://doi.org/10.1029/1998GL900307, 1999.

Hersbach, H., Bell, B., Berrisford, P., Hirahara, S., Horányi, A., Muñoz-Sabater, J., Nicolas, J., Peubey, C., Radu, R., Schepers, D., et al.: The ERA5 global reanalysis, Quart. J. Roy. Meteorol. Soc., 146, 1999–2049, https://doi.org/10.1002/qj.3803, 2020.

Ingólfsson, O., Illenberger, E., and Schmidt, W.-F.: Photodetachment from anions in a drift at 337nm cell. Application to SF, Int. J. Mass Spectrom., 139, 103–110, https://doi.org/10.1016/0168-1176(94)90020-5, 1994.

Kanakidou, M., Dentener, F. J., and Crutzen, P. J.: A global three-dimensional study of the fate of HCFCs and HFC-134a in the troposphere, Journal of Geophysical Research: Atmospheres, 100, 18 781–18 801, https://doi.org/10.1029/95JD01919, 1995.

https://doi.org/10.5194/egusphere-2025-3597
Preprint. Discussion started: 13 August 2025

Ko, M. K., Sze, N. D., Wang, W.-C., Shia, G., Goldman, A., Murcray, F. J., Murcray, D. G., and Rinsland, C. P.: Atmospheric sulfur hexafluoride: Sources, sinks and greenhouse warming, Journal of Geophysical Research: Atmospheres, 98, 10 499–10 507, https://doi.org/10.1029/93JD00228, 1993.

Kolonjari, F., Sheese, P. E., Walker, K. A., Boone, C. D., Plummer, D. A., Engel, A., Montzka, S. A., Oram, D. E., Schuck, T., Stiller, G. P., et al.: Validation of Atmospheric Chemistry Experiment Fourier Transform Spectrometer (ACE-FTS) chlorodifluoromethane (HCFC-22) in the upper troposphere and lower stratosphere, Atmos. Meas. Tech., 17, 2429–2449, https://doi.org/10.5194/amt-17-2429-2024, 2024.

Kosaka, Y., Kobayashi, S., Harada, Y., Kobayashi, C., Naoe, H., Yoshimoto, K., Harada, M., Goto, N., Chiba, J., Miyaoka, K., et al.: The JRA-3Q reanalysis, Journal of the Meteorological Society of Japan. Ser. II, 102, 49–109, https://doi.org/10.2151/jmsj.2024-004, 2024.

Kouznetsov, R., Sofiev, M., Vira, J., and Stiller, G.: Simulating age of air and the distribution of SF6 in the stratosphere with the SILAM model, Atmos. Chem. Phys., 20, 5837–5859, https://doi.org/10.5194/acp-20-5837-2020, 2020.

Kovács, T., Feng, W., Totterdill, A., Plane, J. M., Dhomse, S., Gómez-Martín, J. C., Stiller, G. P., Haenel, F. J., Smith, C., Forster, P. M., García, R. R., Marsh, D. R., and Chipperfield, M. P.: Determination of the atmospheric lifetime and global warming potential of sulfur hexafluoride using a three-dimensional model, Atmos. Chem. Phys., 17, 883–898, https://doi.org/10.5194/acp-17-883-2017, 2017.

Krey, P., Lagomarsino, R., and Toonkel, L.: Gaseous halogens in the atmosphere in 1975, J. Geophys. Res., 82, 1753–1766, https://doi.org/10.1029/JC082i012p01753, 1977.

Laeng, A., Plieninger, J., Von Clarmann, T., Grabowski, U., Stiller, G., Eckert, E., Glatthor, N., Haenel, F., Kellmann, S., Kiefer, M., et al.: Validation of MIPAS IMK/IAA methane profiles, Atmos. Meas. Tech., 8, 5251–5261, https://doi.org/10.5194/amt-8-5251-2015, 2015.

Li, Q., Fernandez, R. P., Hossaini, R., Iglesias-Suarez, F., Cuevas, C. A., Apel, E. C., Kinnison, D. E., Lamarque, J.-F., and Saiz-Lopez, A.: Reactive halogens increase the global methane lifetime and radiative forcing in the 21st century, Nat. Commun., 13, 2768, https://doi.org/10.1038/s41467-022-30456-8, 2022.

Lin, S.-J. and Rood, R. B.: Multidimensional flux-form semi-Lagrangian transport schemes, Monthly weather review, 124, 2046–2070, https://doi.org/10.1175/1520-0493(1996)124<2046:MFFSLT>2.0.CO;2, 1996.

Loeffel, S., Eichinger, R., Garny, H., Reddmann, T., Fritsch, F., Versick, S., Stiller, G., and Haenel, F.: The impact of sulfur hexafluoride (SF6) sinks on age of air climatologies and trends, Atmos. Chem. Phys., 22, 1175–1193, https://doi.org/10.5194/acp-22-1175-2022, 2022.

McLandress, C. and Shepherd, T. G.: Simulated anthropogenic changes in the Brewer-Dobson circulation, including its extension to high latitudes, J. Climate, 22, 1516–1540, https://doi.org/10.1175/2008JCLI2679.1, 2009.

Meinshausen, M., Vogel, E., Nauels, A., Lorbacher, K., Meinshausen, N., Etheridge, D. M., Fraser, P. J., Montzka, S. A., Rayner, P. J., Trudinger, C. M., Krummel, P. B., Beyerle, U., Canadell, J. G., Daniel, J. S., Enting, I. G., Law, R. M., Lunder, C. R., O'Doherty, S., Prinn, R. G., Reimann, S., Rubino, M., Velders, G. J., Vollmer, M. K., Wang, R. H., and Weiss, R.: Historical greenhouse gas concentrations for climate modelling (CMIP6), Geosci. Model Dev., 10, 2057–2116, https://doi.org/10.5194/gmd-10-2057-2017, 2017.

Minschwaner, K., Hoffmann, L., Brown, A., Riese, M., Müller, R., and Bernath, P.: Stratospheric loss and atmospheric lifetimes of CFC-11 and CFC-12 derived from satellite observations, Atmos. Chem. Phys., 13, 4253–4263, https://doi.org/10.5194/acp-13-4253-2013, 2013.

Moore, D. P. and Remedios, J. J.: Growth rates of stratospheric HCFC-22, Atmos. Chem. Phys., 8, 73–82, https://doi.org/10.5194/acp-8-73-2008, 2008.

Morris, R. A., Miller, T. M., Viggiano, A. A., Paulson, J. F., Solomon, S., and Reid, G.: Effects of electron and ion reactions on atmospheric lifetimes of fully fluorinated compounds, https://doi.org/10.1029/94JD02399, 1995.

Patra, P., Takigawa, M., Dutton, G., Uhse, K., Ishijima, K., Lintner, B., Miyazaki, K., and Elkins, J.: Transport mechanisms for synoptic, seasonal and interannual SF 6 variations and" age" of air in troposphere, Atmos. Chem. Phys., 9, 1209–1225, 2009.

https://doi.org/10.5194/egusphere-2025-3597
Preprint. Discussion started: 13 August 2025

Ploeger, F., Legras, B., Charlesworth, E., Yan, X., Diallo, M., Konopka, P., Birner, T., Tao, M., Engel, A., and Riese, M.: How robust are stratospheric age of air trends from different reanalyses?, Atmos. Chem. Phys., 19, 6085–6105, https://doi.org/10.5194/acp-19-6085-2019, 2019.

Prather, M. J. and Holmes, C. D.: A perspective on time: Loss frequencies, time scales and lifetimes, Environ. Chem., 10, 73–79, https://doi.org/10.1071/EN13017, 2013.

Prather, M. J., Froidevaux, L., and Livesey, N. J.: Observed changes in stratospheric circulation: decreasing lifetime of N_2O, 2005–2021, Atmos. Chem. Phys., 23, 843–849, https://doi.org/10.5194/acp-23-843-2023, 2023.

Prignon, M.: Stratospheric circulation changes: investigations using multidecadal observations and simulations of inorganic fluorine, Ph.D. thesis, ULiège - Université de Liège, 2021.

Prignon, M., Chabrillat, S., Friedrich, M., Smale, D., Strahan, S., Bernath, P. F., Chipperfield, M., Dhomse, S., Feng, W., Minganti, D., et al.: Stratospheric fluorine as a tracer of circulation changes: Comparison between infrared remote-sensing observations and simulations with five modern reanalyses, Journal of Geophysical Research: Atmospheres, 126, e2021JD034 995, https://doi.org/10.1029/2021jd034995, 2021.

Ravishankara, A. R., Solomon, S., Turnipseed, A. A., and Warren, R. F.: Atmospheric Lifetimes of Long-Lived Halogenated Species, pp. 194–199, https://doi.org/10.1126/science.259.5092.194, 1993.

Ray, E. A., Moore, F. L., Elkins, J. W., Rosenlof, K. H., Laube, J. C., Röckmann, T., Marsh, D. R., and Andrews, A. E.: Quantification of the SF6 lifetime based on mesospheric loss measured in the stratospheric polar vortex, J. Geophys. Res., 122, 4626–4638, https://doi.org/10.1002/2016JD026198, 2017.

Reddmann, T., Ruhnke, R., and Kouker, W.: Three-dimensional model simulations of SF6 with mesospheric chemistry, Journal of Geophysical Research Atmospheres, 106, 14 525–14 537, https://doi.org/10.1029/2000JD900700, 2001.

Reed, R. J.: The present status of the 26-month oscillation, Bull. Amer. Meteorol. Soc., 46, 374–387, 1965.

Saunders, L. N., Walker, K. A., Stiller, G. P., von Clarmann, T., Haenel, F., Garny, H., Bönisch, H., Boone, C. D., Castillo, A. E., Engel, A., et al.: Age of air from ACE-FTS measurements of sulfur hexafluoride, Atmos. Chem. Phys., 25, 4185–4209, https://doi.org/10.5194/acp-25-4185-2025, 2025.

Shangguan, M. and Wang, W.: Analysis of temperature Semi-Annual Oscillations (SAO) in the middle atmosphere, Remote Sensing, 15, 857, https://doi.org/10.3390/rs15030857, 2023.

Sheese, P. E., Walker, K. A., Boone, C. D., Bernath, P. F., Froidevaux, L., Funke, B., Raspollini, P., and von Clarmann, T.: ACE-FTS ozone, water vapour, nitrous oxide, nitric acid, and carbon monoxide profile comparisons with MIPAS and MLS, J. Quant. Spectrosc. Radiat. Transfer, 186, 63–80, https://doi.org/10.1016/j.jqsrt.2016.06.026, 2017.

SPARC: SPARC Report on the Lifetimes of Stratospheric Ozone-Depleting Substances, Their Replacements, and Related Species. M.K.W. Ko, P.A. Newman, S. Reimann, S.E. Strahan (Eds.), SPARC Report No. 6, WCRP-15/2013, available at urlwww.sparc-climate.org/publications/sparc-reports/, 2013.

SPARC: The SPARC Data Initiative: Assessment of stratospheric trace gas and aerosol climatologies from satellite limb sounders, Tech. Rep. 8, SPARC, https://www.sparc-climate.org/publications/sparc-reports/, wCRP-5/2017, 2017.

SPARC: SPARC Reanalysis Intercomparison Project (S-RIP) Final Report, Tech. Rep. 10, SPARC, https://doi.org/10.17874/800dee57d13, 2022.

https://doi.org/10.5194/egusphere-2025-3597
Preprint. Discussion started: 13 August 2025

Spivakovsky, C., Logan, J., Montzka, S., Balkanski, Y., Foreman-Fowler, M., Jones, D., Horowitz, L., Fusco, A., Brenninkmeijer, C., Prather, M., et al.: Three-dimensional climatological distribution of tropospheric OH: Update and evaluation, Journal of Geophysical Research: Atmospheres, 105, 8931–8980, https://doi.org/10.1029/1999JD901006, 2000.

Strahan, S. and Polansky, B.: Meteorological implementation issues in chemistry and transport models, Atmos. Chem. Phys., 6, 2895–2910, https://doi.org/10.5194/acp-6-2895-2006, 2006.

Totterdill, A., Kovács, T., Martín, J. C. G., Feng, W., and Plane, J. M.: Mesospheric Removal of Very Long-Lived Greenhouse Gases SF6 and CFC-115 by Metal Reactions, Lyman-α Photolysis, and Electron Attachment, J. Phys. Chem. A, 119, 2016–2025, https://doi.org/10.1021/jp5123344, 2015.

Voet, F., Ploeger, F., Laube, J., Preusse, P., Konopka, P., Grooß, J.-U., Ungermann, J., Sinnhuber, B.-M., Höpfner, M., Funke, B., Wetzel, G., Johansson, S., Stiller, G., Ray, E., and Hegglin, M. I.: On the estimation of stratospheric age of air from correlations of multiple trace gases, 25, 3541–3565, https://doi.org/10.5194/acp-25-3541-2025, 2025.

Volk, C. M., Elkins, J. W., Fahey, D. W., Dutton, G. S., Gilligan, J. M., Loewenstein, M., Podolske, J. R., Chan, K. R., and Gunson, M. R.: Evaluation of source gas lifetimes from stratospheric observations, Journal of Geophysical Research Atmospheres, 102, 25 543–25 564, https://doi.org/10.1029/97jd02215, 1997.

Wang, Y., Huang, D., Liu, J., Zhang, Y., and Zeng, L.: Alternative Environmentally Friendly Insulating Gases for SF6, Processes, 7, https://doi.org/10.3390/pr7040216, 2019.

Waugh, D. W. and Hall, T. M.: Age of stratospheric air: Theory, observations, and models, Rev. Geophys., 40, 1–1–1–26, https://doi.org/10.1029/2000RG000101, 2002.